Table 1 Viscosities (mean ± 95% confidence intervals) of clean and slicked surface microlayers and corresponding bulkwaters, measured by fluorescence depolarization techniques at 21.2 °C

Date	Location	Bulkwater (mPa s)	Clean surface (mPa s)	Slicked surface (mPa s)
14 August	Oregon	1.030 ± 0.011	1.029 ± 0.014	1.054 ± 0.024
25 August	Oregon	1.044 ± 0.007	1.039 ± 0.009	1.055 ± 0.007
	same	1.043 ± 0.007	1.043 ± 0.003	1.093 ± 0.016
17 Sept.	Maine	1.057 ± 0.003	1.061 ± 0.007	1.097 ± 0.007
	same	1.055 ± 0.007	1.066 ± 0.007	1.281 ± 0.007
18 Sept.	Maine	1.055 ± 0.007	1.059 ± 0.018	1.070 ± 0.016
	same	1.055 ± 0.008	1.064 ± 0.003	1.078 ± 0.007
25 Sept.	Florida	1.081 ± 0.017	1.082 ± 0.017	
	same	1.075 ± 0.005	1.067 ± 0.016	1.092 ± 0.005

Locations, dates, and original water temperatures: Oregon—Yaquina Bay, 14 and 25 August 1986, 13.5 °C; Maine—Damariscotta Estuary, 17 and 18 September 1986, 14.0 °C; Florida—off Tampa Bay, 25 September 1986, 29.5 °C. All salinities were ≥30‰. Microlayer samples, collected with a glass plate, had sample thicknesses of 40–60 μm (volume collected per dip/plate area). Bulkwaters were sampled at 20 cm depths. Samples were stored in silanized glass vials and returned to Oregon for depolarization measurements.

between microlayer viscosity and enrichment of UV-absorbing materials (microlayer absorbance/bulkwater absorbance)[8] but the absorbant materials passed 0.2-μm filters while the viscous materials generally did not. An appropriate model for composition and formation of viscous microlayers may include effects such as polymers have on solution properties. As little as 0.05 wt% of certain organic polymers can result in full gelation[13]; increased viscosity has been observed in non-gelling agarose solutions at solute volume fractions as small as 0.05% (ref. 14). Organic carbon in oceanic microlayers is in the range 0.001–0.01 wt% (taking microlayer total organic carbon as 5–50 mg l (ref. 15) and assuming the materials were 50% carbon). The disparity between amounts measured on the ocean surface and amounts required for laboratory gelation is only slight considering that: (1) microlayer viscosities sufficient to modify surface waves may be only a fraction of gel viscosities; (2) microlayer components such as proteins may have enhanced volumes due to orientation near the interface[16]; and (3) microlayers can also be enriched in major cations[17] and trace metals[18,19] whose effects may be to bridge and thereby extend the influence of individual organic molecules.

The presence of viscous microlayers seems to violate a central assumption of monolayer models, which is that bulk properties such as viscosity are constant right up to the actual interface[1]. Monolayer models also consider interfacial films as newtonian liquids, but the presence of filterable materials in the microlayer samples and their contribution to microlayer viscosity may indicate non-newtonian properties in the interfacial region[20]. It may be possible to assign microlayer viscosity to the surface as a component of surface shear or surface dilational viscosity[21], or it may be necessary to include explicit terms for vertical and horizontal dissipation between upper and lower boundaries of the microlayer[22], terms which are considered negligible or ignored in monolayer models[23]. The viscosities measured were intrinsic volume properties of the natural microlayer samples, evident without spreading or compressing the samples at an interface. As such, the microlayer viscosities are distinct from vicinal water theories[24] which require compressed monolayer films to induce near-surface viscosity.

Models for gas[25], momentum[26] and heat exchange[27] across the air-sea interface all invoke viscous microlayers, as so-called stagnant films or thermal or viscous sublayers, of dimensions similar to depths of microlayers sampled here. It is evident from the data presented here that, in slicks at least, the viscosity of those sublayers may be considerably greater than subsurface viscosity. The importance of such viscosity enhancements on air-sea exchange depends on the extent of surface slick conditions. The extent of viscous slick conditions will also influence emissivity of the ocean surface: relaxation times of water itself[28] and of solutes such as proteins[29] increase directly with viscosity. Increased relaxation times in viscous microlayers will decrease dielectric constants and brightness temperatures[30], effects previously attributed to long-distance ordering induced by monolayer films[31]. It is clear that discussion and investigation of interfacial properties and processes must be expanded to include consideration of viscous microlayers.

Thanks to L. Mayer, J. Paul and M. DeFlaun for help in sampling, to L. Morrill and J. Brophy for the analyses and to John C. Scott for a very thorough and constructive review. This work supported by the Office of Naval Research.

Received 9 March; accepted 9 September 1987.

1. Lucassen-Reynders, E. H. & Lucassen, J. *Adv. Colloid Interface Sci.* **2**, 347-395 (1969).
2. Ermakov, S. A. *et al. Dynam. Atmos. Oceans* **10**, 31-50 (1986).
3. Pogorzelski, S., Linde, B. & Sliwinski, A. *Acoust. Lett.* **8**, 5-9 (1984).
4. Williams, P. M. *et al. Mar. Chem.* **19**, 17-98 (1986).
5. Hunter, K. A. & Liss, P. S. in *Marine Organic Chemistry* (eds Duursma, E. K. & Dawson, R.) 259-298 (Elsevier, Amsterdam, 1981).
6. Daumas, R. A., Laborde, P. L., Marty, J. C. & Saliot, A. *Limnol. Oceanogr.* **21**, 319-326 (1976).
7. Carlson, D. J. *Mar. Chem.* **11**, 189-208 (1982).
8. Carlson, D. J. *Nature* **296**, 426-429 (1982).
9. Rotman, A. & Heldman, J. *Biochemistry* **20**, 5995-5999 (1981).
10. Fuchs, P., Parola, A., Robbins, P. W. & Booth, E. R. *Proc. natn. Acad. Sci. U.S.A.* **72**, 3351-3354 (1975).
11. Carlson, D. J., Morrill, L. E. & Brophy, J. E. *Limnol. Oceanogr.* (in the press).
12. Chen, R. F. & Bowman, R. L. *Science* **147**, 729-732 (1965).
13. Sinclair, M., Lim, K. C. & Heeger, A. J. *Phys. Rev. Lett.* **51**, 1768-1771 (1983).
14. Letherby, M. R. & Young, D. A. *J. chem. Soc. Faraday Trans.* **77**, 1953-1966 (1981).
15. Carlson, D. J. *Limnol. Oceanogr.* **28**, 415-431 (1983).
16. MacRitchie, F. *Adv. Colloid Interface Sci.* **25**, 341-385 (1986).
17. Pattenden, N. J., Cambray, R. S. & Playford, K. *Geochim. cosmochim. Acta* **45**, 93-100 (1981).
18. Barker, D. R. & Zeitlin, H. *J. geophys. Res.* **77**, 5076-5086 (1972).
19. Hardy, J. T., Apts, C. W., Crecelius, E. A. & Bloom, N. S. *Est. Coastal Shelf Sci.* **20**, 299-312 (1985).
20. Jenkinson, I. R. *Nature* **323**, 435-437 (1986).
21. Ting, L., Wasan, D. T., Miyano, K. & Xu, S.-Q. *J. Colloid Interface Sci.* **102**, 248-259 (1984).
22. Mordashev, V. I. & Cherkesov, L. V. *Izvestia Atmos. Ocean Phys.* **22**, 306-310 (1986).
23. Goodrich, F. C. *J. phys. Chem.* **66**, 1858-1863 (1962).
24. Huhnerfuss, H. & Alpers, W. *J. phys. Chem.* **87**, 5251-5258 (1983).
25. Liss, P. S. *Deep-Sea Res.* **20**, 221-238 (1973).
26. Wu, J. *J. phys. Oceanogr.* **14**, 138-144 (1984).
27. Paulson, C. A. & Simpson, J. J. *J. geophys. Res.* **86**, 11044-11054 (1981).
28. Collie, C. H., Hasted, J. B. & Ritson, D. M. *Proc. Phys. Soc.* **60**, 145-160 (1948).
29. Hasted, J. B. *Aqueous Dielectrics* (Chapman & Hall, London, 1973).
30. Maul, G. A. *Introduction to Satellite Oceanography* (Nijhoff, Dordrecht, Netherlands, 1985).
31. Alpers, W., Blume, H.-J. C., Garrett, W. D. & Huhnerfuss, H. *Int. J. Remote Sensing* **3**, 457-474 (1982).

Chernobyl radionuclides in a Black Sea sediment trap

K. O. Buesseler,*, H. D. Livingston*, S. Honjo*
B. J. Hay*, S. J. Manganini*, E. Degens†,
V. Ittekkot†, E. Izdar‡ & T. Konuk‡

* Woods Hole Oceanographic Institution, Woods Hole, Massachusetts 02543, USA
† Geologisch Paläontologisches Institut, Universität Hamburg, D-2000 Hamburg 13, FRG
‡ Dokuz Eylül Üniversitesi, Deniz Bilimleri ve Teknolojisi Enstitüsü, Izmir, Turkey

The Chernobyl nuclear power station accident[1–3] released large quantities of vaporized radionuclides, and, to a lesser extent, mechanically released small (<1–10 μm) aerosol particles[2,4]. The total release of radioactivity is estimated to be of the order of $1–2 \times 10^{18}$ Bq ($3–5 \times 10^{7}$ Ci) not allowing for releases of the xenon and krypton gases[2]. The ^{137}Cs releases of 3.8×10^{16} Bq from Chernobyl can be compared to 1.3×10^{18} Bq ^{137}Cs released due to atmospheric nuclear weapons testing[1]. Chernobyl-derived radionuclides can be used as transient tracers to study physical and biogeochemical processes. Initial measurements of fallout Chernobyl radionuclides from a time-series sediment trap at 1,071 m

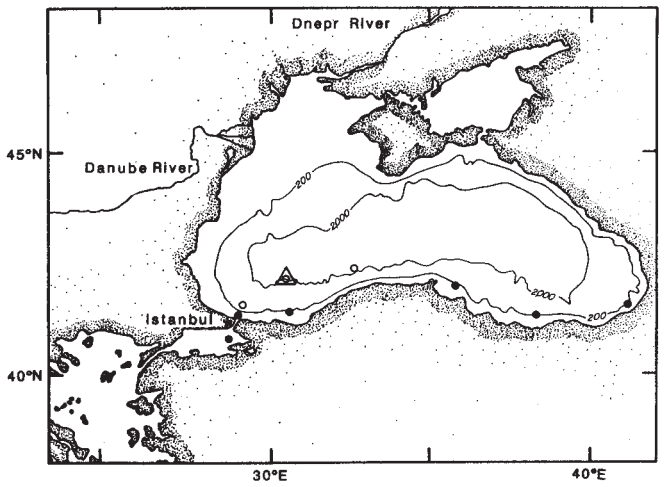

Fig. 1 Location map for Black Sea samples. The triangle marks the sediment-trap site. The open and filled circles represent the location of surface-water samples for particulate and dissolved radionuclides. The open circles are deep stations (>200 m), while the filled circles are shelf stations (<200 m). Depth contours are in m.

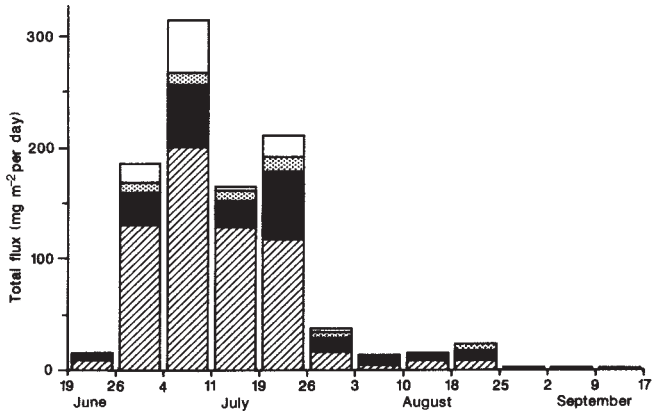

Fig. 2 Total flux (in mg m^{-2} per day) of settling particles found in each sampling cup between 19 June and 17 September 1986. Each flux bar is divided into the percentage of lithogenic, carbonate and biogenic silica found in the sample. ▨, Carbonate; ■, organic carbon; ▩, biogenic silica; □, lithogenics.

during June–September 1986 in the southern Black Sea are presented. The specific activities of ^{137}Cs, ^{144}Ce and ^{106}Ru in the trap samples (0.5–2, 4–12 and 6–13 Bq g^{-1}) are independent of the particle flux while their relative activities reflect their rates of scavenging in the order Ce > Ru > Cs.

The Black Sea is the closest salt-water body to the Chernobyl reactor site and is also connected to the accident site by the Dnepr River. Fallout radioactivity was likely to have been deposited to the Black Sea predominantly during the later stages of the Chernobyl accident (1–6 May)[5]. Chernobyl fallout in southern Europe[6] and the Black Sea region is more enriched in the refractory radionuclides such as ^{144}Ce and ^{106}Ru, relative to the more volatile ^{131}I and ^{137}Cs (which were more abundant in the fallout releases before May[4,6]). Elevated ^{134}Cs and ^{137}Cs levels in June in the surface waters of the southern Black Sea[7] confirm the existence of widespread direct atmospheric deposition of fallout from the Chernobyl accident to this basin. With time, runoff from the Danube and Dnepr Rivers will provide an additional indirect source of Chernobyl radioactivity for this basin.

The Black Sea is a unique water body in that the surface oxic waters (which extended down to 120 m at the trap site in September) are underlain by a large basin of permanently anoxic deep water. These two layers are separated by a strong density gradient between the brackish surface waters and the more saline deep waters.

A time-series sediment trap[8] with a 1.2-m^2 aperture was deployed from the RV *K. Piri Reis* at 41°51.22′ N, 30°21.15′ E (Fig. 1) at a depth of 1,071 m along a bottom-tethered mooring array (anchor depth 2,100 m). The trap collected settling particles over 12 equal intervals of 7.5 days each, from 20 June to 18 September 1986. The sample-receiving cups were poisoned with formaldehyde to inhibit biological activity. The trap was immediately redeployed for further monitoring of the radionuclide flux. Upon recovery, the sample-collection cups were sealed and transported to Woods Hole where they were kept under refrigeration. The following Chernobyl radionuclides were detected by non-destructive gamma spectrometry: ^{134}Cs, ^{137}Cs, ^{141}Ce, ^{144}Ce, ^{103}Ru, ^{106}Ru, ^{95}Nb, and ^{110m}Ag (with 6–18 h counting intervals in the energy range of 134–884 keV). The detector-counting rates were calibrated with a ^{152m}Eu solution standard. All activities are corrected for decay to 1 May 1986. The presence of short-lived ^{141}Ce, ^{103}Ru, ^{95}Nb and ^{134}Cs/^{137}Cs activity ratio of 0.5 (characteristic of Chernobyl fallout) in the trap material allowed us to positively identify the radioactivity flux as resulting from the recent Chernobyl releases.

The total sediment-trap flux increased from 19 mg m^{-2} per day in June to a maximum of 360 mg m^{-2} per day during the week of 4–11 July 1986. The flux remained high throughout July, decreased in August, and dropped off to <3 mg m^{-2} per day in September. This seasonal peak in particle flux is consistent with previous sediment-trap studies at a nearby site[9] and is due to the high productivity of the coccolithophorid species, *Emiliania huxleyi*. The trap material in the bloom period consists of >60% calcium carbonate, and is composed primarily of coccoliths (Fig. 2). In contrast to other periods of the year[9], the flux of biogenic silica and lithogenic particles is relatively low during the sampling period (Fig. 2).

The radiochemical data (Table 1 and Figs 3 and 4) are given for ^{134}Cs, ^{137}Cs, ^{144}Ce and ^{106}Ru as these radionuclides were readily detected by the gamma-spectrometry technique, and their half-lives are long enough to allow the study of their environmental geochemistry over a period of a few to several tens of years ($t_{1/2}$ = 2.07, 30.17, 0.78 and 1.02 yr, respectively). To facilitate reference to other studies, we report here our mean ^{103}Ru/^{106}Ru and ^{141}Ce/^{144}Ce ratios to be 4.80 ± 0.07 and 1.44 ± 0.06, respectively. The specific activities of ^{137}Cs, ^{144}Ce and ^{106}Ru in the trap samples contrast sharply with the total flux pattern and are not identical for each isotope (Fig. 3 and Table 1). The specific activity of ^{137}Cs decreases slightly from ≈2 Bq g^{-1} (dry weight) to <1 Bq g^{-1} between June and August. The ^{144}Ce specific activity in mid-June is 6.2 Bq g^{-1}, increasing systematically to a peak of almost 12 Bq g^{-1} at the end of July, and then rapidly decreasing to the 4–5 Bq g^{-1} level. The ^{106}Ru specific activity is roughly constant at 7 Bq g^{-1} with a single point activity maximum in late August. The mechanism responsible for these trends is not reflected in the patterns shown in total mass and other sedimentary components (compare Figs 2 and 3). The lack of correlation between trap flux and specific activity is consistent with other studies of particle reactive elements[10,11] and reflects, at least partially, a constant exchange equilibrium between the dissolved and particulate phases. This equilibrium is between the dissolved phase, the suspended particulate (small) and settling particulate (large) phases. Radionuclides exchange reversibly between the dissolved and suspended phases, and the suspended and settling particulate phases exchange by aggregration/disaggregation. Hence, the radionuclide flux is proportional to the settling particle flux. The total radionuclide fluxes are driven by the much larger seasonal variation in primary productivity, which is reflected in the large flux of biogenic components during the first half of the sampling period (Table 1).

The ^{134}Cs/^{137}Cs, ^{144}Ce/^{137}Cs and ^{106}Ru/^{137}Cs ratio data can

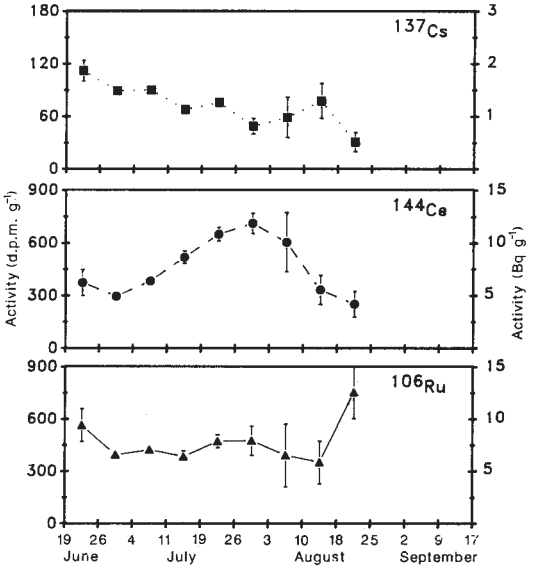

Fig. 3 Sediment trap ^{137}C, ^{144}Ce and ^{106}Ru specific activities against time for the sediment-trap material collected between 19 June and 17 September 1986 (data in Table 1). The dates on the *x*-axis are the opening and closing dates for the sediment-trap sample cups. The activity scales are given as d.p.m. g^{-1} on the left vertical axis and as Bq g^{-1} on the right vertical axis (60 d.p.m. = 1 Bq). The error bars indicate the analytical error given in Table 1 and are drawn if larger than the symbol.

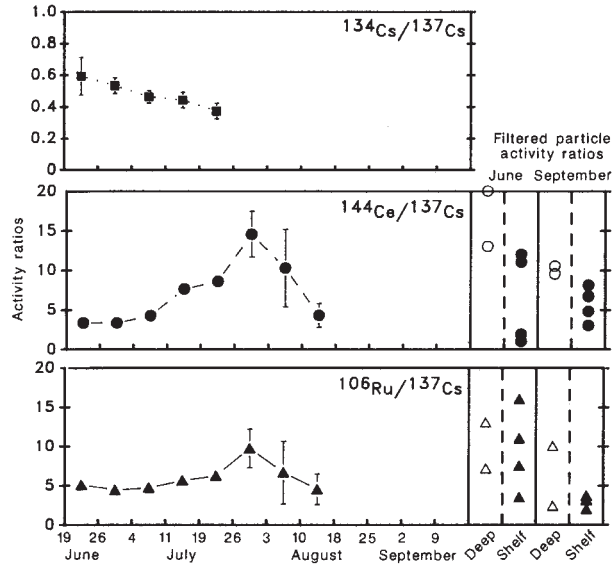

Fig. 4 The sediment-trap $^{134}Cs/^{137}Cs$, $^{144}Ce/^{137}Cs$ and $^{106}Ru/^{137}Ca$ activity ratios against time. The ratios shown are from the first 5–8 samples in the time series only, as the error on the activity ratios (drawn as an error bar around the data points) becomes unacceptably large in the later samples which had the lowest sample masses (see Table 1). For ^{144}Ce and ^{106}Ru, where the radionuclide activity on the filtered particles (>0.45 μm) is substantial, their filtered particle activity ratios are also shown for comparison on an extension to the right-hand side of the graphs. In each case, the ratio data from the filtered particles are given from the June (left) and September (right) cruises and from surface waters collected at deep (open symbols) and shelf (filled symbols) stations (see Fig. 1 for station locations).

be used to examine the relative scavenging chemistries of Cs, Ce and Ru (Fig. 4). There are two sources of fallout Cs in the Black Sea: Chernobyl fallout with its characteristic $^{134}Cs/^{137}Cs$ ratio of ~0.5, and pre-existing atmospheric nuclear weapons fallout with a $^{134}Cs/^{137}$ Cs ratio of zero (due to ^{134}Cs decay since the major bomb inputs in the 1960s). The $^{134}Cs/^{137}Cs$ ratio in the trap material decreases with time from an initial value of ~0.5 to <0.440. This decrease in the $^{134}Cs/^{137}Cs$ ratio and the total ^{137}Cs activity with time indicates that the percentage of Chernobyl ^{137}Cs, relative to global fallout ^{137}Cs is decreasing in the trap material during this collection period.

The $^{144}Ce/^{137}Cs$ ratio in the sediment-trap samples (Fig. 4) peaks around the end of July, reflecting the strong trend in Ce specific activity discussed previously. In Fig. 4, the $^{144}Ce/^{137}$ Cs ratio of the trap material is compared to the $^{144}Ce/^{137}Cs$ ratio we have found in filtered particles (>0.45 μm) collected in the surface waters of the Black Sea. If we consider the fine particles which are collected in the overlying surface waters as being the source of the larger aggregates found in the trap, or at least as being similar in the particle-to-solution partitioning, then two features should be noted. First, the range of $^{144}Ce/^{137}Cs$ ratios found in the fine particles and sediment-trap samples is similar. Second, the surface-water particulate $^{144}Ce/^{137}Cs$ ratios vary, depending upon their location, such that the $^{144}Ce/^{137}Cs$ ratios of the shelf stations are lower than those at the deeper stations. This is apparently due to increased Ce removal in the more

Table 1 Black Sea sediment trap at 1,071 m, 41°51.22′ N; 30°21.15′ E

Trap collection dates (1986)	Total flux mg m^{-2} day^{-1}	Specific activity (Bq g^{-1})* ^{137}Cs	^{144}Ce	^{106}Ru	Radionuclide flux (Bq m^{-2} per day) ^{137}Cs	^{144}Ce	^{106}Ru
19–26 June	18.9	1.9±0.2	6.2±1.2	9.4±1.6	0.04	0.12	0.18
26 June–5 July	231.1	1.5±0.08	5.0±0.3	6.6±0.5	0.34	1.15	1.52
4–11 July	356.9	1.5±0.08	6.4±0.3	7.1±0.5	0.54	2.28	2.52
11–19 July	184.7	1.1±0.08	8.7±0.6	6.4±0.6	0.21	1.60	1.18
19–26 July	230.9	1.3±0.08	10.9±0.6	7.9±0.6	0.29	2.51	1.82
26 July–3 August	45.8	0.8±0.2	11.9±0.9	7.9±1.4	0.04	0.54	0.36
3–10 August	15.2	1.0±0.4	10.1±2.8	6.5±3.0	0.01	0.15	0.10
10–18 August	16.2	1.3±0.3	5.6±1.4	5.9±2.1	0.02	0.09	0.09
18–25 August	30.3	0.5±0.2	4.2±1.2	12.6±2.5	0.02	0.13	0.38
25 August–2 September	2.7	1.9±1.4	8.2±5.6	9.0±10.3	0.01	0.02	0.02
2–9 September	2	BD	BD	BD	—	—	—
9–17 September	1.4	BD	BD	BD	—	—	—
			Annual flux (Bq m^{-2} yr^{-1}) =		46.0	261.1	248.7

* Specific activities as Bq g^{-1} dry weight, with one standard deviation counting error. All activities are decay corrected to 1 May 1986.
BD, below detection (due to low sample mass).
Estimated inventories of Chernobyl ^{137}Cs, ^{144}Ce and ^{106}Ru (data taken from our Black Sea Chernobyl studies[13]): Mean ^{137}Cs, ^{144}Ce, and ^{106}Ru activities in surface water are 170, 8, and 10 Bq m^{-3}, respectively. Penetration of ^{137}Cs into water column is 35 m (assume the same for ^{144}Ce and ^{106}Ru). Total inventories of ^{137}Cs, ^{144}Ce, and ^{106}Ru are 6.0×10^3, 2.8×10^2, and 3.5×10^2 Bq, respectively. Removal rate: Inventory/annual flux, ^{137}Cs = 130 years, ^{144}Ce = 1.1 years, ^{106}Ru = 1.4 years.

coastal sites (see Fig. 1 for location of shelf and deep-water stations). As the settling time of the sinking coccoliths is of the order of two weeks to reach 1,071 m[9], particles collected in the trap will not have been formed in the surface waters directly above the trap site due to rapid circulation of Black Sea surface waters (0.1–0.3 m s^{-1}, ref. 12). Therefore, an increase in the $^{144}Ce/^{137}Cs$ ratio could reflect a shift in the source of the trap particles from shelf to deeper sites. If, in general, the $^{144}Ce/^{137}Cs$ ratio is lowered in the surface waters due to continued Ce scavenging, then a longer trap record should show an overall decrease in the $^{144}Ce/^{137}Cs$ ratio with time.

The $^{106}Ru/^{137}Cs$ ratios in the sediment-trap material do not vary substantially and are within the range of the fine particle $^{106}Ru/^{137}Cs$ ratios (Fig. 4*b*). While Ru is more particle reactive than Cs, it is less particle reactive than Ce in the surface waters (the particulate/soluble ratios for ^{137}Cs, ^{106}Ru and ^{144}Ce are ~0.1%, 4% and 11%, respectively, at this trap site in September)[13,14] Consistent with this trend in particle reactivity (Cs < Ru < Ce), we have found that the relative enrichment of Ru on the trap material is less than that of Ce when compared to their total activities in the surface waters[13,14].

The trap-radionuclide fluxes can be compared to estimated water column Chernobyl-fallout inventories to examine the relative removal rates of each radionuclide. The removal time of Chernobyl ^{137}Cs (130 y) is much longer than that of ^{106}Ru and ^{144}Ce (1.4 and 1.1 yr, respectively, see Table 1). The latter could be an upper limit if significant amounts of Ce or Ru are soluble in the deep anoxic waters. The total ^{137}Cs flux measured over the first three months following Chernobyl is therefore rather small relative to the total ^{137}Cs inventory. The more particle-reactive Ru and Ce are being much more rapidly removed from the surface Black Sea, as expected by their affinity for the particulate phases. Relative particle-reactivity trends for Ce and Ru may be indicated better from the partition between particulate/soluble phases than from their removal-time estimates. The former approach does not require the added assumption of the association of observed particle fluxes with water-column inventories in September.

The initial sediment-trap results indicate that there was rapid removal of a considerable fraction of the Chernobyl radionuclides to the deep Black Sea. The more soluble isotope ^{137}Cs is less efficiently removed from the surface waters at this deep trap site than are the more particle-reactive isotopes, ^{144}Ce and ^{106}Ru. Future radiochemical analyses of ^{90}Sr (a highly soluble tracer) and the Pu, Am and Cm isotopes (particle-reactive tracers) in the trap samples will provide an additional range of contrasting geochemistries for comparison.

Coupled with water-column and sediment studies, the time-series sediment-trap record will allow us to determine the geochemical fate of recently introduced Chernobyl radionuclides in the Black Sea. Also, this work will have further important implications for understanding the geochemistries of a wide variety of naturally occurring chemical analogues in this unique oceanographic setting.

We thank our scientific colleagues for their cooperation, and the US National Science Foundation, the US Office of Naval Research, the Coastal Research Center at Woods Hole, the German Minister for Research and Technology, and the Scientific and Technical Research Council of Turkey for financial assistance. The officers and crew of the *K. Piri Reis* were invaluable in their assistance in deploying the sediment-trap mooring, and in sampling the Black Sea waters on two cruises in 1986. We thank our co-workers W. R. Clarke and S. A. Casso for their assistance in sample collection and radiochemistry. This is contribution number 6473 from the Woods Hole Oceanographic Institution.

Received 4 May; accepted 13 August 1987.

1. Levi, B. G. *Physics Today* December, 17-20 (1986).
2. *Summary Report on the Post-Accident Review Meeting on the Chernobyl Accident.* Safety Series No. 75-INSAG-1 (IAEA, Vienna, 1986).
3. Hohenemser, C. *et al. Environment* **28,** 6-13, 30-43 (1986).
4. Devell, L. *et al. Nature* **321,** 192-193 (1986).
5. Alexandropoulos, N. G. *et al. Nature* **322,** 779 (1986).
6. Krey, P. W. *US Department of Energy Report EML-460* 155-213 (US Department of Energy, Environmental Measurements Laboratory, New York, 1986).
7. Livingston, H. D. *et al. US Department of Energy Rep. EML-460,* 214-223 (US Department of Energy, Environmental Measurements Laboratory, New York, 1986).
8. Honjo, S. & Doherty, K. *Deep Sea Res.* (in the press).
9. Honjo, S. *et al. Particle Flux in the Ocean, Mitteil. Geol. Pal. Inst.* Vol. 62 (eds Degens, E. T., Izdar, E. & Honjo, S.) (University of Hamburg, in the press).
10. Bacon, M. P., Huh, C.-A., Fleer, A. P. & Deuser, W. G. *Deep Sea Res.* **32,** 273-286 (1985).
11. Fowler, S. W. & Knauer, G. A. *Progr. Oceanog.* **16,** 147-194 (1986).
12. Zentovitch, V. T. in *The Encyclopedia of Oceanography, Encyclopedia of Earth Science Series* Vol. 1 (ed. Fairbridge, R. W.) 145-150 (Halsted, New York, 1966).
13. Livingston, H. D. & Buesseler, K. O. *Eos* **67,** 1070 (1986).
14. Livingston, H. D., Buesseler, K. O., Izdar, E. & Konuk, T. *Proc. Int. Symp. on Radioactivity and Oceanography* (Elsevier, in the press).

Chernobyl nuclide record from a North Sea sediment trap

S. Kempe* & H. Nies†

* Geologisch-Paläontologisches Institut, University of Hamburg, Bundesstrasse 55, D-2000 Hamburg 13, FRG
† Deutsches Hydrographisches Institut, Bernhard-Nocht-Strasse 78, D-2000 Hamburg 4, FRG

Nuclides liberated by explosion and subsequent fire at Chernobyl No. 4 reactor on 26 April 1986, travelled to Western Europe with lower tropospheric air masses[1]. They reached the northern Alps[2] and Paris[3] on 30 April, southern Great Britain[4] on 2 May, the southern North Sea[5] on 3 May, and the northern North Sea[1] on 3 May and again on 8 May. Levels of deposited activity varied by a factor of 30 or more over distances <100 km because of variability of rainfall[2,6]. A sediment trap deployed 222-m-deep in the North Sea off Bergen recorded the onset and magnitude of the deposition of Chernobyl nuclides. The trap collected 13 samples between 24 April and 21 September 1986. The flux of nuclides adsorbed to particles sinking from surface waters to sediments started less than ten days after contaminated air reached the site. Maximum specific activity occurred on 16–27 May for ^{137}Cs, ^{134}Cs, ^{106}Ru and ^{103}Ru, and on 8–20 June for ^{144}Ce, ^{95}Nb and ^{95}Zr. The highest activity was found for ^{103}Ru. The highest total specific activity of these nuclides in depositing sediments reached 670,000 Bq kg^{-1}, and the highest total activity flux for one day amounted to 50 Bq m^{-2}.

A sediment trap recorded the onset and magnitude of the nuclide flux from the North Sea surface to sediments; it was stationed 30 nautical miles (1.852 km) off Bergen at the western side of the Norwegian Channel (60° 29.6′ N, 3° 50.4′ E, water depth 318 m). The Mark-VI Honjo sediment trap[7] was moored at a water depth of 222 m, well below the summer thermocline. Its 0.509-m^2 opening directed the settling particles into cups, which were automatically advanced at preprogrammed dates (interval 11.62 days during deployment NS III, summer 1986). The cups were filled with saturated NaCl- solution and poisoned with $HgCl_2$. The first cup was opened on 24 April and the last was closed on 20 September 1986 (Table 1). The trap and samples were recovered by the German RV *Valdivia*, and the samples were transported undisturbed and cooled.

The samples were investigated for Chernobyl nuclides on 20–27 October by gamma-spectroscopy at the DHI. Original sample cups were placed directly on the Ge(Li)-detectors. The energy-dependent efficiency calibration was done with a nuclide mixture of the Physikalisch-Technische-Bundesanstalt, which contained known activities of ^{7}Be, ^{54}Mn, ^{57}Co, ^{65}Zn, ^{88}Y, ^{133}Ba, ^{137}Cs and ^{139}Ce. It was assumed that all of the activity was adsorbed to settled sediment covering the bottom of the cups and had not dissolved to any extent in the overlying NaCl-solution. This assumption was later tested with filtered sediment. Both measurements delivered comparable (decay-corrected) results, suggesting that, in fact, all of the measured activity was bound to particles. The counting time for samples N3 to N10